

# Development of a novel test-setup for identifying the frictional characteristics of carbon fibre reinforced polymer composites at high surface pressure

Prateek Saxena<sup>1</sup>, Marie Schinzel<sup>2</sup>, Manuela Andrich<sup>2</sup> and Niels Modler<sup>2</sup>

<sup>1</sup> Industrial Tribology Machine Dynamics & Maintenance Engineering Centre (ITMMEC), Indian Institute of Technology Delhi, New Delhi, India

<sup>2</sup> Technische Universität Dresden, Institut für Leichtbau und Kunststofftechnik (ILK), 01062 Dresden, Germany

E-mail: pra.9000@gmail.com

**Abstract.** Carbon fibre reinforced polymer composites are extensively used in industrial applications. They are light in weight and have excellent load bearing properties. To understand this material's behaviour when carrying loads at high pressure, a tensile-friction test device was developed that can apply a contact surface pressure between composite and counterpart of 50-300 MPa. A tribological investigation of carbon fibre reinforced epoxy composites was carried out, in which the influence of the surface morphology was investigated by using grinding and sandblasting techniques. The friction coefficient of the polymer composite was measured at 100 MPa surface pressure against uncoated and Diamond-Like Carbon coated stainless steel counterparts.

## 1. Introduction

Carbon Fibre Reinforced Polymer (CFRP) composites are increasingly used as high-performance composites. In an assembly together with other parts, composite materials are loaded at contact surfaces and bearing areas where there is localised high specific pressure and movement at low speeds. In such cases, it is important to determine the friction behaviour of the surfaces in relative motion. The coefficient of friction depends on many factors, namely speed, pressure, temperature, material surfaces etc. Faure et al. [1] examined the friction and wear behaviour of titanium alloys (Ti-6Al-4V) against steel and other counterparts using a special tribometer. In the pressure range of 36.1MPa - 38.9MPa and low sliding velocity conditions, frictional heat generated led to softening of the surface which caused further wear of the titanium alloys.

The coefficient of friction for surfaces in contact can be either static or dynamic in nature. When a tangential force is applied to the surface, a transition period exists before actual motion begins. In this region, a static coefficient of friction exists which changes to the dynamic coefficient of friction when actual motion starts [2, 3]. To perform tribometric analysis of the surfaces, tribometers are designed specifically for the particular condition. Dunkin and Kim [3] used a Centrifugal Friction Apparatus for their studies to measure the coefficient of static friction for flat surfaces experiencing low loading conditions.



Another setup for studying friction was demonstrated by Pougis et al. [4]. A study to investigate the friction of steel was performed at a low sliding velocity under dry conditions. To realise high contact pressure between 350 MPa – 1 GPa a pin of diameter 5 mm was used as specimen. Carbon fibre reinforced polymer composites are incapable of sustaining this pressure range in combination with high shear forces. To perform friction studies on carbon composites in the range of 50MPa-250MPa, it was necessary to develop a device that could perform friction studies at high pressure without disturbing the structure of the composite.

In this experimental work, a new test setup was developed to measure the coefficient of friction of polymer composites against coated and uncoated steel counterparts at high surface pressure and relatively low sliding velocities. The tribological behaviour of CFRP composites was analysed at high surface pressure ranging between 50 MPa to 300 MPa. Since the pressure required is moderately high in comparison to the metallic surfaces; specimens of dimensions 5 mm X 20 mm X 3 mm were used. The effectiveness of the setup was validated by preparing different surfaces using grinding and sandblasting techniques on polymer composites before performing the friction studies on them. The static and dynamic coefficient of friction was determined for each specimen against uncoated and Diamond-Like Carbon (DLC) coated steel counterparts.

## 2. Methods

The tribological tests for measuring the coefficient of friction ( $\mu$ ), called tensile-friction-test, were conducted using a specially developed test setup in combination with a commercially-available universal tensile testing machine (Zwick/Röll). This test device made it possible to investigate the material behavior of the test specimen at high surface pressure and low relative velocity.

### 2.1. Tensile-Friction test setup

The setup of the tensile-friction-test device is shown in figure 1. By the upper clamping and the lower roughened part of the friction bar, the test device is fixed centrally in the hydraulic jaws of the universal tensile testing machine. The two fastening bolts, on each of which two strain gauges were glued, were used for the defined application and measurement of the required normal force. The four strain gauges were joined in a Wheatstone bridge and connected to a measuring amplifier for signal processing. The software of the measuring amplifier makes it possible to convert and evaluate the measured strains of the strain gauges directly in terms of applied force. To determine the interrelation between exerted force and measured strains and to allow this transformation, the calibration of the strain gauges in a tensile test is required. For this purpose, the fastening bolts were clamped by means of specimen holder bars in the tensile testing machine and loaded with a defined force.

The setting of the normal force was performed by adjusting the nuts on the rear part of each fastening bolt. When these nuts are tightened the disc spring assembly in front is tensioned. Via the disc spring assembly, which is included to compensate for small irregularities and shape deviations on the specimen holder and the friction bar, the introduced force of each fastening bolt is transmitted through the mounting brackets and onto the sample holders. This structural design of the test device makes it possible to tighten the springs until the required normal force value is displayed on the measuring amplifier. Here it should be noted, that the required normal force  $F_N$  is composed of the sum total of the individual force on each fastening bolt  $F_{B1}$  and  $F_{B2}$  (individual strain on both bolts):

$$F_N = F_{B1} + F_{B2} \quad (1)$$

In each specimen holder two parallel cut-outs were located on the side facing the friction bar, in to which the four test specimens were inserted. As a result of the normal force, the test specimens were pressed against the friction bar, whereby a local pressure load was created in the contact area between the specimens and the friction bar. By moving the upper traverse of the tensile testing machine, the friction bar was pulled out of the test device. This tensile force  $F_T$  causes a friction load in the contact surface between friction bar and specimen and is determined by a load cell integrated in the tensile

testing machine as the friction force  $F_F$ . The biaxial stress caused by normal force  $F_N$  and friction force  $F_F$  (figure 2) can be presented by the following relationship:

$$\mu = F_F / F_N \tag{2}$$

where  $\mu$  is the coefficient of friction between the sliding pair

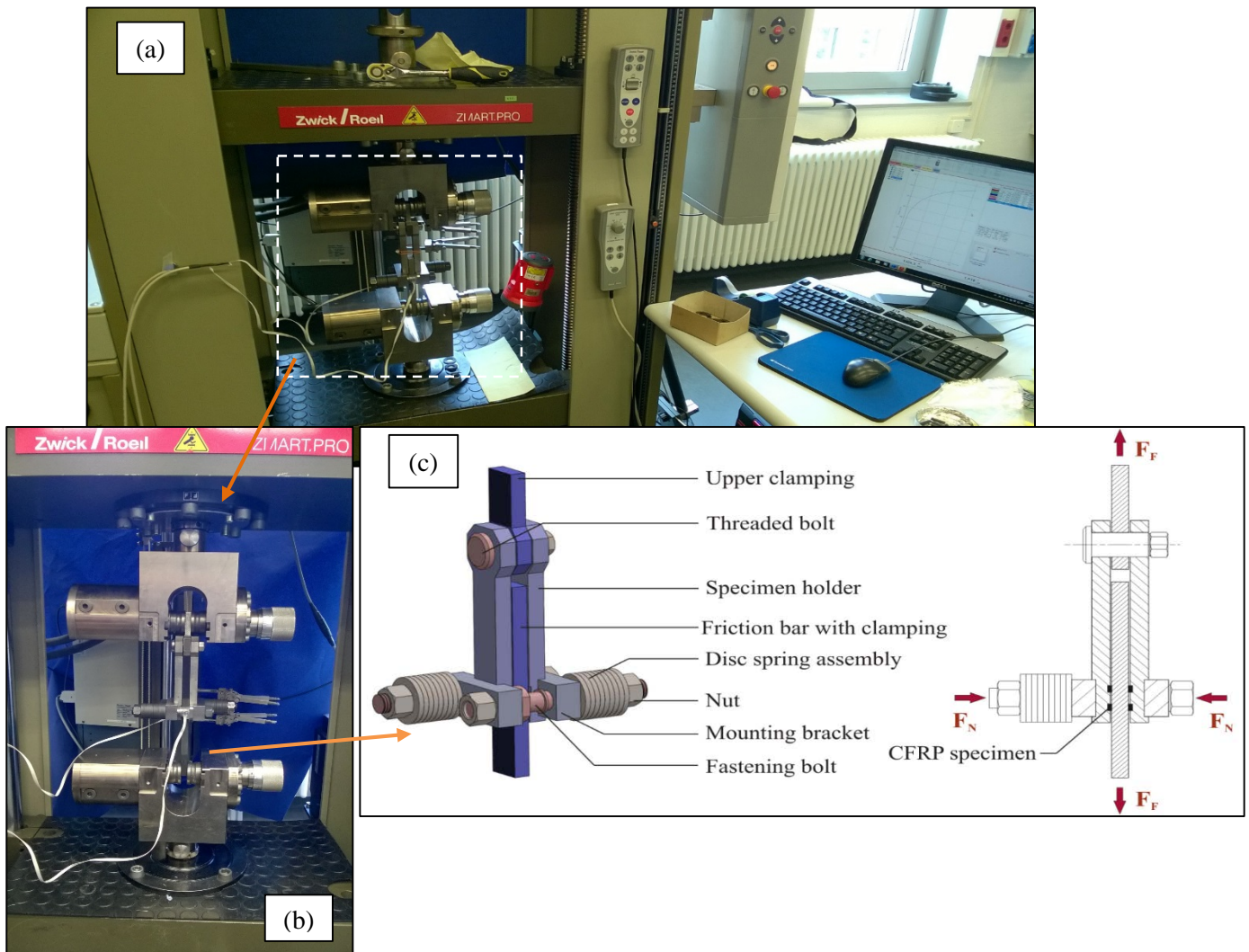


Figure 1: (a) Test setup for tensile-friction testing of CFRP composites, (b) Enlarged view of the device and (c) Schematic diagram of the tensile-friction test setup

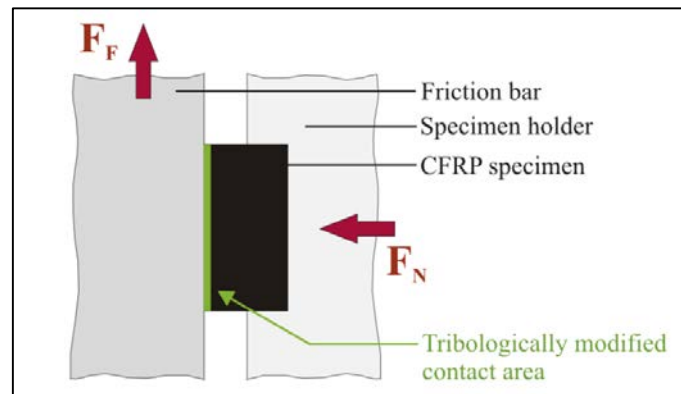


Figure 2: Forces in the contact zone between test specimen and friction bar

Due to the action of the friction force, a shear load was generated in the contact surface between friction bar and test specimens. The shear load was initiated by exceeding the limit value of static friction  $\mu_s$  and thereby moving to dynamic friction  $\mu_d$ . The curve progression of the friction force  $F_F$  is shown in principle in the diagram in figure 3. The front part of the curve is characterised by a linearly rising behaviour, which illustrates the range of static friction  $\mu_s$ . The specimens exhibited elastic yield. At the limit value of  $\mu_{s,max}$  (indicated by the red circle) the shear load can no longer be compensated elastically, which results in a relative movement of the friction partners and dynamic friction behaviour. Because of the changing and increasing linear progression of the dynamic friction  $\mu_d$ , a mixed friction mode can be assumed. This leads to a sliding movement and shearing of the surfaces against each other in the tribologically modified contact surface.

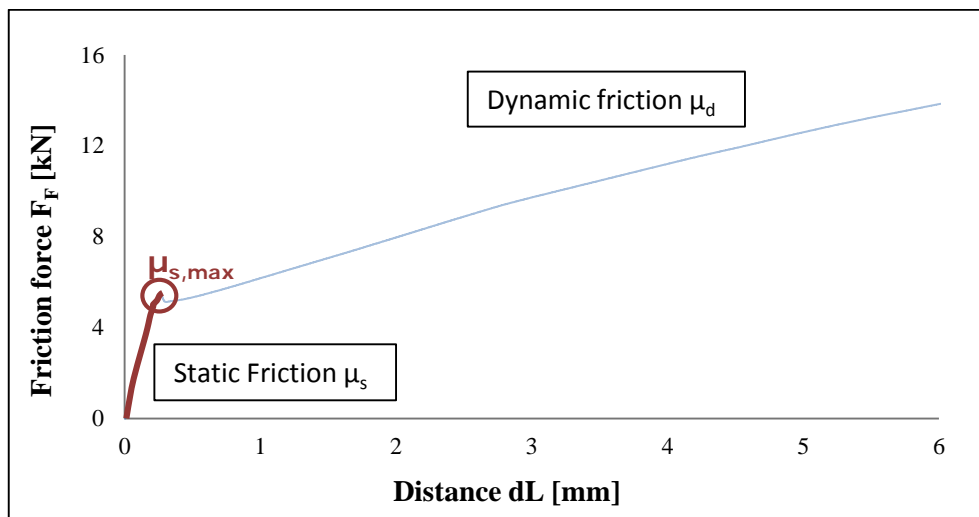


Figure 3: A typical friction force curve

Owing to the resulting wear on the test specimens, the friction bar must be made sufficiently long. The specimens move over only one section of the friction bar per trial and the friction bar can then be used for several test procedures. The distance traversed is termed the standard travel distance  $dL$  and corresponds to the traverse path of the tensile testing machine. Due to the dimension of each test specimen (5 x 20 x 3 mm) the friction test obtained an average over the set of 4 specimens with a total test area of 400 mm<sup>2</sup>.

In general, the tensile-friction-test was influenced by the material properties of the specimens and the friction bar, the surface roughness, the lubricant, the testing temperature, the selected pressure and the testing speed. From the measured parameters of the test the coefficient of static friction  $\mu_s$  can be determined for the investigated friction pairings by using the following calculation:

$$\mu_s = \mu_{s,max} / F_N \quad (3)$$

A subsequent optical investigation of the tribologically stressed contact surface of the specimens and the friction bar by a profilometry technique, was used to perform a detailed analysis of the wear and a determination of the surface roughness.

### 3. Experimental Investigations

#### 3.1. Material

The friction pairings experimentally investigated in this study were CFRP composites against uncoated and DLC-coated stainless steel. The composite material for the CFRP test specimens was a bidirectional woven carbon fabric: Torayca style 896 (satin weave 1/4, build by T800HB carbon fibres with a density in warp and weft direction of 1.81 g/cm<sup>2</sup>) infused with the mono-component epoxy resin Hexflow® RTM6-2 (Co. Hexcel Composites GmbH & Co. KG) by advanced Resin Transfer Moulding (RTM) process [5]. RTM 6 as a thermoset matrix resin is used in components for lightweight applications, and especially for aerospace structures. It is characterised by a high glass transition temperature, short curing cycles, ease of processing, low moisture absorption, excellent wetting properties and good mechanical properties. The service temperature ranges from -60 °C to 180 °C. The fibre volume fraction was about 57 % with a cure cycle of 75 min at 160 °C in mould and a post cure cycle of 120 min at 180 °C.

The friction bars as counterparts were made of stainless heat-treated steel type C45, which is characterised by high tensile strength and good ductility. For a variation of the experimental investigations the tests were performed both with uncoated and with DLC-coated friction bars. This method of surface coating with a DLC layer has special properties, such as extreme hardness (about 4000 HVN [6]), high load resistance and resistance to abrasive and adhesive wear, excellent sliding properties and chemical stability [7], which is why this kind of surface coating is often used in a wide range of tribo-applications, according to a review by Alan H. Lettington [8].

#### 3.2. Surface Preparation

The surfaces of the test specimens were prepared with different surface treatment techniques to attain the required surface characteristics [9]. In the current study, grinding and sandblasting were selected as suitable methods for surface modification. Several strips with the size of 5 mm width and about 120 mm length were cut from the RTM-plate. The surface of each polymer strip was treated using one of the two techniques with adjusted parameter configurations to generate different roughness and afterwards cut into the required size of the specimen with a length of 20 mm. of these four test specimens were used in the tensile-friction-test.

*3.2.1. Grinding.* For surface preparation, grinding sandpaper with silicon carbide (SiC) abrading particles was used, with three different grit sizes: 40, 120 and 240. The test specimen strips were manually and gently rubbed backwards and forwards against the abrasive paper in one direction for about 2 minutes. This generated three different sets of test specimens with uniformly roughened surfaces, all rougher than the surface of the reference specimen Ref ( $Ra_{Ref} = 0.677 \mu\text{m}$ ). According to the Coated Abrasive Manufacturing Institute (CAMI) grit designation, the grit size 40 causes a coarse, grit size 120 a fine and grit size 240 a very fine surface roughness. It can be concluded that with increasing grit size, the abrasiveness of silicon carbide paper decreases. The surface prepared from abrasive paper of grit size 240 was therefore relatively smooth compared to the surface prepared

with grit size 40. This is apparent in the images made with the optical microscope (figure 4):  $G_{40}$  ( $Ra_{G_{40}} = 3.11 \mu\text{m}$ ),  $G_{120}$  ( $Ra_{G_{120}} = 2.38 \mu\text{m}$ ) and  $G_{240}$  ( $Ra_{G_{240}} = 1.16 \mu\text{m}$ ).

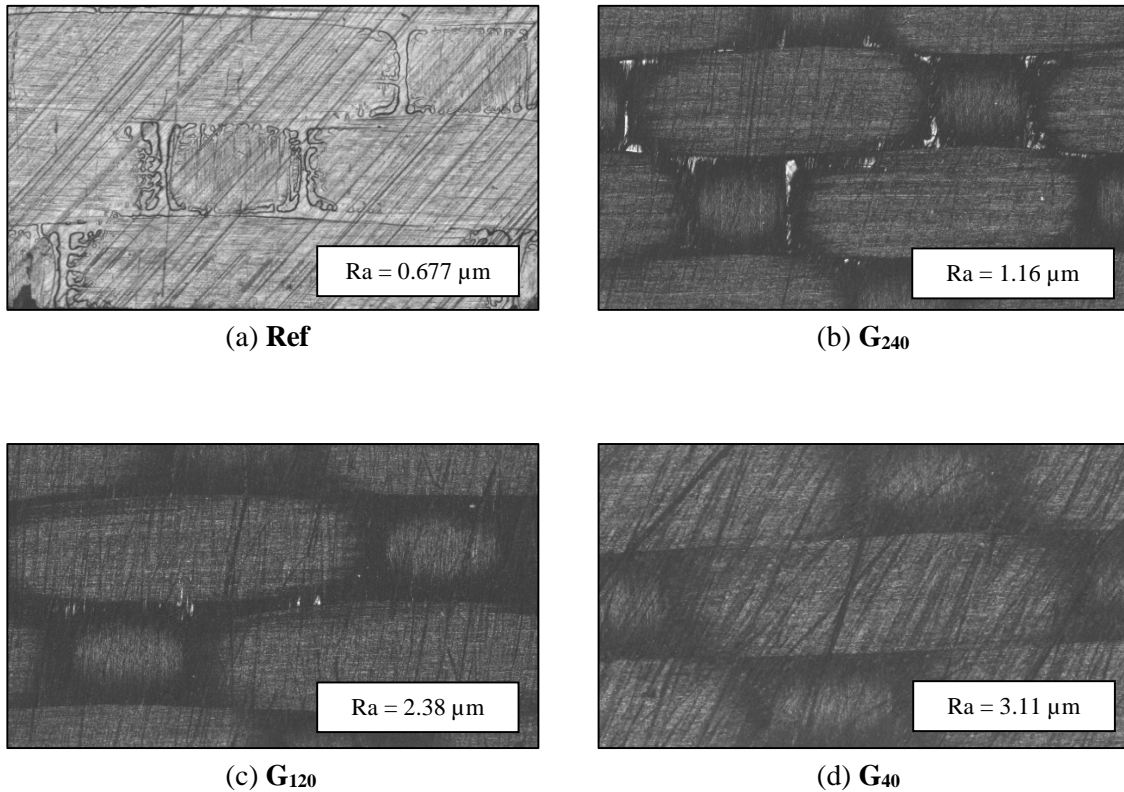


Figure 4: Different roughened surfaces by grinding: (a) Reference specimen Ref, (b) Surface prepared with abrasive paper of grit size 240  $\mu\text{m}$   $G_{240}$ , (c) grit size 120  $\mu\text{m}$   $G_{120}$  and (d) grit size 40  $\mu\text{m}$   $G_{40}$

**3.2.2. Sandblasting.** A surface preparation of the CFRP test specimens was performed by using a blasting agent under high pressure. In this study, glass balls were used as the abrasive material. These particles, with uniform size, diameter and shape, generate a uniform roughness of the surface. In addition to the type of the abrasive material, the impact angle, the diameter of the particles, the level of air pressure, the distance between the surface of the sample and the blasting tip and the duration of blasting all influence the roughness of the sandblasted surface. During the sandblasting procedure in this test, the impact angle was always  $90^\circ$ , the distance about 10 cm and the duration was about 5 min. The different configurations of sandblasting with varying pressure (from 1.5 bar to 2.5 bar) and diameter of the glass particle (from 40  $\mu\text{m}$  minimum to 400  $\mu\text{m}$  maximum) are shown in Table 1.

Table 1: Configuration of surface preparation using sand blasting

Name	Pressure (bar)	Impact angle ( $^\circ$ )	Abrasive material	Diameter ( $\mu\text{m}$ )	Ra ( $\mu\text{m}$ )
Ref	-	-	-	-	0.677
SB <sub>40</sub>	1.5	90	Glass ball	40 - 70	0.592
SB <sub>150</sub>	2	90	Glass ball	150 - 250	0.694
SB <sub>300</sub>	2.5	90	Glass ball	300 - 400	1.28

These three configurations for sandblasting surfaces were used in the present study to obtain different types of roughened surface. As illustrated in figure 5, sandblasting leads on one hand to an increase of the surface roughness ( $SB_{300}$ ), but also on the other hand to a refinement of the surface ( $SB_{40}$ ) compared to the reference Ref ( $Ra_{Ref} = 0.677 \mu\text{m}$ ). The surface of the  $SB_{300}$  test specimen, processed with a pressure of 2.5 bar and the largest diameter size of the glass particles, shows the highest roughness value obtained by sandblasting ( $Ra_{SB_{300}} = 1.28 \mu\text{m}$ ). This is evident from the fact that with increasing value of the applied pressure and with increasing size of the abrasive particles, the roughness of the surface increased.

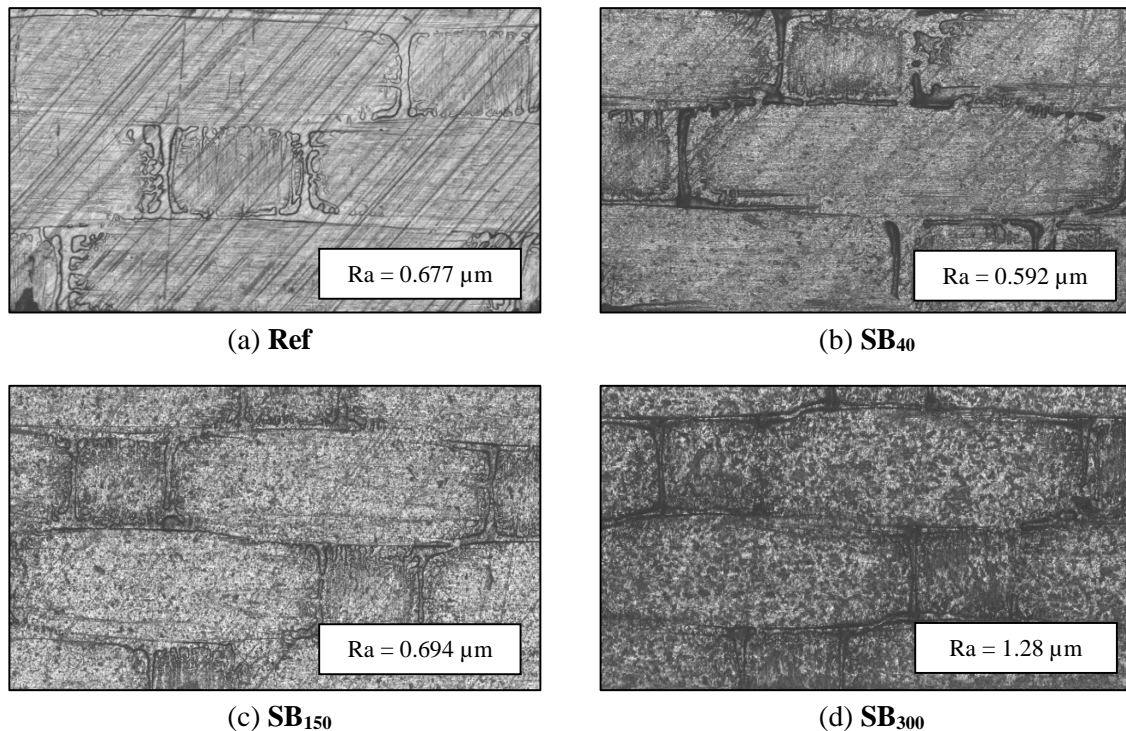


Figure 5: Different roughened surfaces by sandblasting: (a) Reference specimen Ref, (b) Surface prepared from sandblasting at 1.5 bar pressure  $SB_{40}$ , (c) at 2 bar pressure  $SB_{150}$  and (d) at 2.5 bar pressure  $SB_{300}$

### 3.3. Test conditions

The tensile-friction-tests were carried out at a constant pressure in the contact area of  $100 \text{ N/mm}^2$ , which was adjusted by tightening the nuts of the fastening bolts with a normal force of  $F_N = 40 \text{ kN}$ . The friction bar (of coated and uncoated steel) was pulled out of the test device with a testing speed of  $2 \text{ mm/min}$ . The standard travel distance for each test was  $6 \text{ mm}$ . The tests were performed under standard environment test conditions (room temperature at  $25 \text{ }^\circ\text{C}$ , humidity of  $50 \%$ ). No lubricant was used in these investigations.

## 4. Results and Discussion

From the measured friction force curves the friction behaviour for the respective pairings was determined. The limit values of static friction are shown in figure 6 and 7 for the ground and sandblasted friction pairings of CFRP against DLC-coated and uncoated steel. In general, the different surface treatments of the test specimens and the DLC-coating of the friction bar all influenced the friction behaviour.

In all of the friction-tensile-tests the coefficient of static friction ( $\mu_s$ ) with DLC-coated counterparts was higher than when they were uncoated. It can thus be assumed that in the friction tests with a DLC-friction bar a higher friction force must be applied for converting static friction into dynamic friction. The deviation in the reference specimen was about 66 %. In both the ground and sandblasted specimens this measured coefficient of static friction varied between 35 % and 50 %, and the largest difference was found in the friction pairing with the smoothest surface of the CFRP test specimens: DLC/G<sub>240</sub> and DLC/SB<sub>40</sub>.

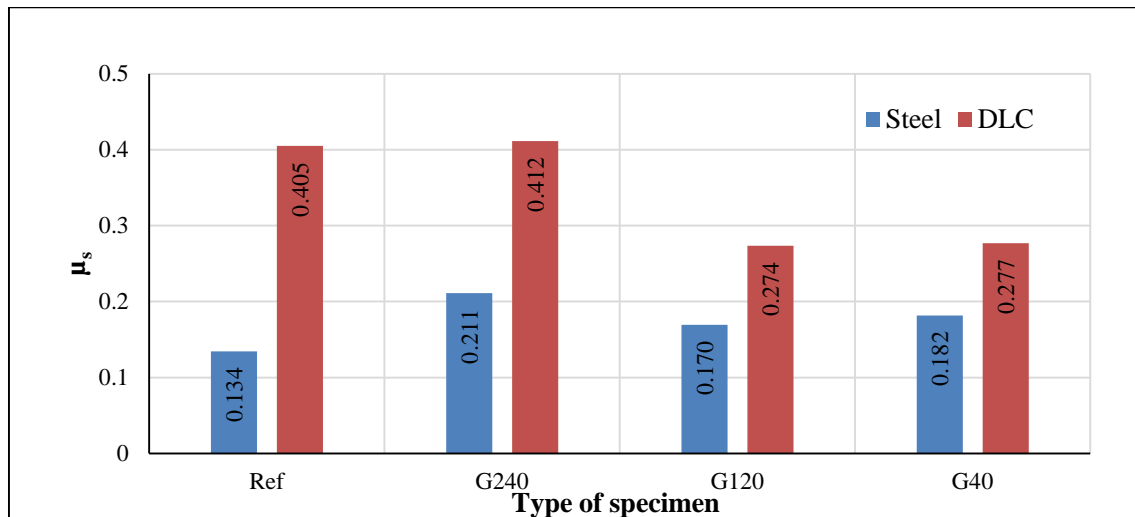


Figure 6: Coefficient of static friction ( $\mu_s$ ) of the investigated grinding CFRP test specimens: G240, G120 and G40 compared to the reference Ref

The ground specimens G<sub>120</sub> and G<sub>40</sub> show almost the same coefficients of friction ( $\mu_s = 0.27$ ) in tribological contact with the DLC-coated counterpart, whereas the value obtained for G<sub>240</sub> was similar to the reference value ( $\mu_s = 0.4$ ). The coefficients of friction of the ground CFRP test specimen against the stainless steel bar were lower and varied only slightly, between 0.17 and 0.21. This phenomenon can also be observed in the sandblasted test specimens. Here, the coefficients of static friction with stainless steel showed only very low variation (between 0.13 and 0.17) among themselves and from the ground test specimens. It may therefore be assumed that the specimens, whether ground or sandblasted, began to slip (initiated dynamic friction behaviour) against the uncoated steel surface at a similar friction force.

On a closer investigation of the friction force, differences in the progression of the respective friction curves were discovered. As shown in figure 8, at the beginning of the test the friction behaviour of the surface treated CFRP against uncoated stainless steel (top row) was characterised by an identical linear slope of the friction force of about 20 % the static friction. At the limit value  $\mu_{s,max}$  the graph has a peak, drops down briefly and then continues to rise, but considerably less rapidly than in the static friction part. The sustained increase in the friction force indicates that there is mixed friction behaviour of dynamic friction and also wear. For all sandblasted test specimens the slope of the curve in the dynamic friction section was relatively the same, but in parallel offset. The same behaviour was found for the ground specimens. Their curves are even flatter than in the sandblasted graphs, but follow a similar trend. From this it can be concluded, that in friction pairings of CFRP against uncoated steel counterparts the different roughness caused by the same surface preparation simply results in a displacement of the friction curves.

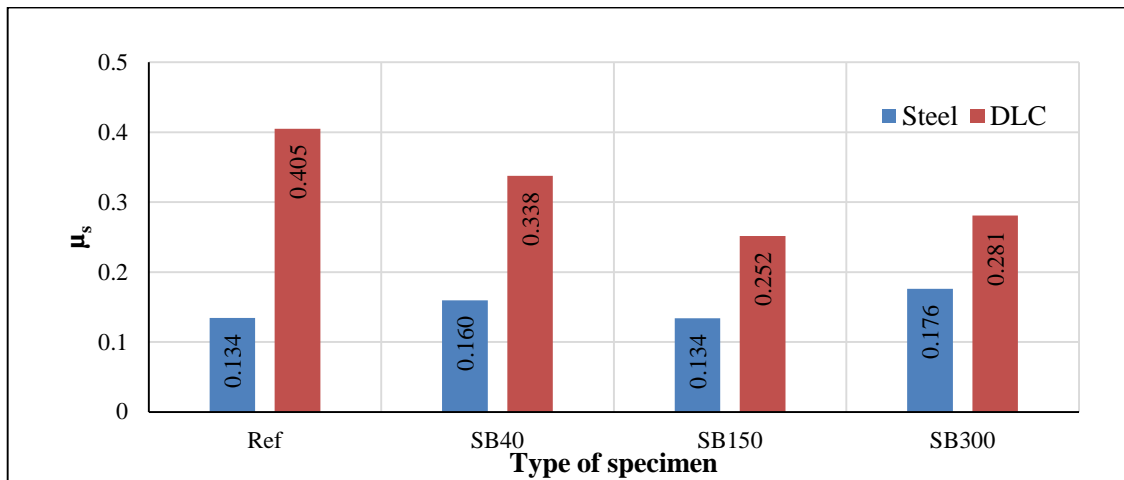


Figure 7: Coefficient of static friction ( $\mu_s$ ) of the investigated sandblasting CFRP test specimens: SB40, SB150 and SB300 compared to the reference Ref

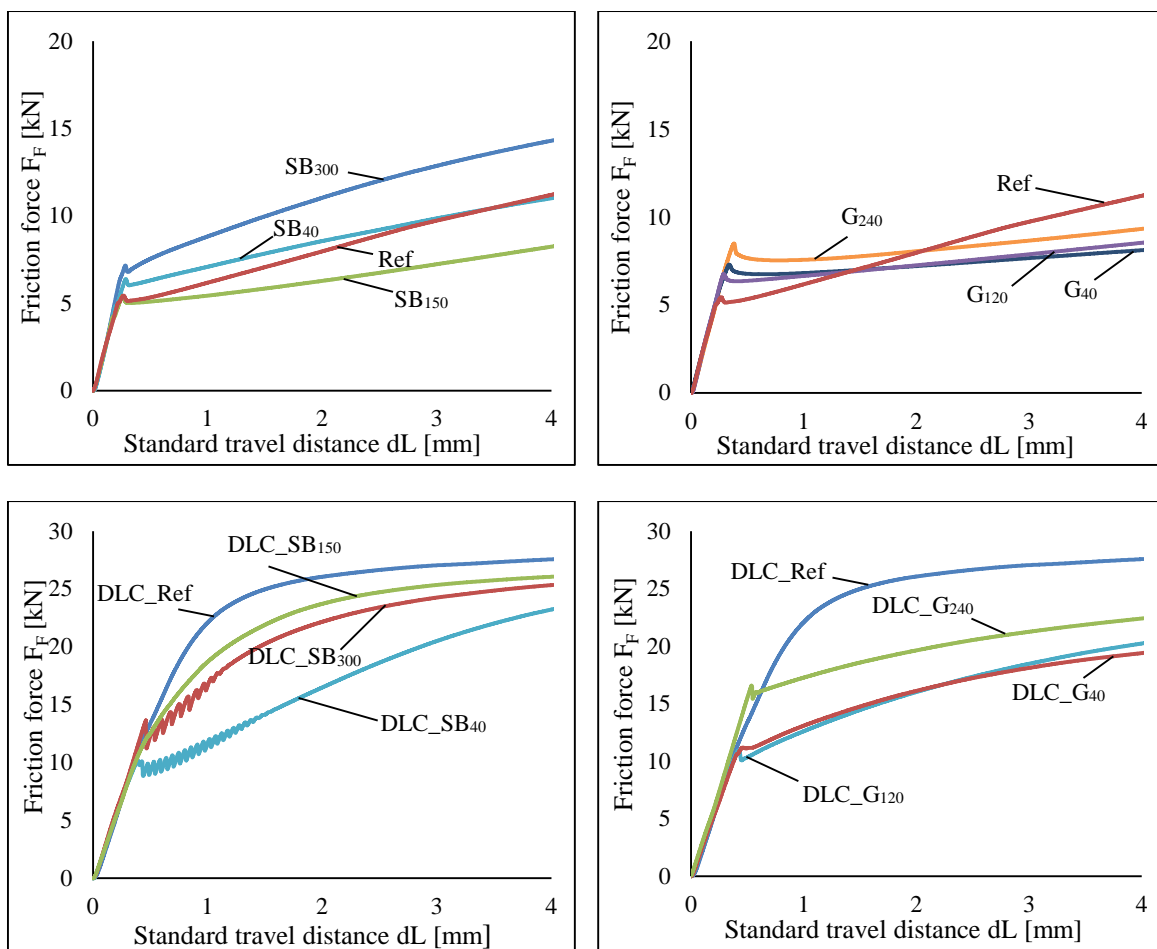


Figure 8: Measured friction force curves  $F_F$  of different surface prepared CFRP test specimen (sand blasting left, grinding right) in tribological contact to uncoated (top row) and DLC-coated friction (bottom row) bars

In contrast, the friction force curves obtained in the DLC-tests were different. For example, the reference specimen in friction pairing with DLC\_Ref shows no peak. In this case, there was a continuous transition from static friction to dynamic friction. As in the dynamic friction part of the curve, the friction force did not increase and a pure sliding behaviour was generated between reference test specimen and DLC-coated friction bar. The test specimens DLC\_SB<sub>300</sub> and DLC\_SB<sub>40</sub> show a different friction behaviour at the onset of dynamic friction, indicated by “jittering” of the curve. This effect is termed a “stick-slip” phenomenon. In this spontaneously jerking motion the static friction in combination with dynamic friction was significantly greater. The alternating sticking and slipping of the surfaces of the friction partners led to more intensive wear of the surfaces.

## 5. Conclusions

The following conclusions can be drawn:

- The coefficient of friction for CFRP specimens against DLC coated steel counterparts was higher than when the counterpart was uncoated.
- The coefficient of friction for the CFRP samples with a roughened surface was 35 % to 50 % greater than was found for the reference specimens.
- The coefficient of static friction for ground CFRP surfaces G<sub>120</sub> and G<sub>40</sub> was the same ( $\mu_s = 0.27$ ) for both counterparts.
- For all of the sandblasted specimens, the changes in the coefficient of dynamic friction were relatively similar but in parallel offset.
- A stick-slip phenomenon was observed when sandblasted samples of CFRP slid against the DLC counterpart.

## 6. Acknowledgements

The authors would like to acknowledge the funding that the Deutsche Forschungs-gemeinschaft (DFG) provides to the Collaborative Research Centre SFB 639 (subprojects B3 and E1) at The Technical University of Dresden. The financial support of DAAD - the German Academic Exchange Service is also acknowledged.

## 7. References

- [1] Faure L., Bolle B., Philippon S., Schuman C., Chevrier P. and Tidu A. 2012 Friction Experiments for titanium alloy tribopairs sliding in dry conditions: Sub-surface and surface analysis *Tribology International* **54** 17–25
- [2] Rabinowicz E. 1951 The nature of the static and kinetic coefficients of friction *Journal of Applied Physics* **22** 1373-9.
- [3] Dunkin JE, Kim DE. 1996 Measurement of static friction coefficient between flat surfaces *Wear* **193** 186-92.
- [4] Pougis A., Philippon S., Massion R., Faure L., Fundenberger J.-J., Toth L.S. 2013 Dry friction of steel under high pressure in quasi-static conditions *Tribology International* **67** 27-35.
- [5] Mills A. 2001 Automation of carbon fibre preform manufacture for affordable aerospace applications *Composites Part A: Applied Science and Manufacturing* **32** 7 955-962.
- [6] Schultrich B, Scheibe H-J, Drescher D, Ziegele H. 1998 Deposition of superhard amorphous carbon films by pulsed vacuum arc deposition *Surface and Coatings Technology* **98** 1097–101.
- [7] Andrich M, Hufenbach W, Kunze K, Scheibe H.-J. 2013 Characterization of the friction and wear behaviour of textile reinforced polymer composites in contact with diamond-like carbon layer *Tribology International* **62** 29-36.
- [8] Lettington A. H. 1998 Applications of diamond-like carbon thin films *Carbon* **36** 555-560.
- [9] Hoffman A. S. 1995 Surface modification of polymers *Chinese Journal of polymer science* **13** 3 195-203.